Title

Evaluating Radioactive Analogs of Doxorubicin to Quantify ChemoFilter Binding and Whole-Body Positron Emission Tomography/Magnetic Resonance Imaging for Drug Biodistribution

Journal

Journal of Vascular and Interventional Radiology, 33(6)

ISSN

1051-0443

Authors

Kumar, Parth
Yee, Colin
Blecha, Joseph E
et al.

Publication Date

2022-06-01

DOI

10.1016/j.jvir.2022.03.007

Peer reviewed

HHS Public Access

Author manuscript

J Vasc Interv Radiol. Author manuscript; available in PMC 2023 June 01.

Published in final edited form as:

J Vasc Interv Radiol. 2022 June ; 33(6): 687–694. doi:10.1016/j.jvir.2022.03.007.

Evaluating Radioactive Analogs of Doxorubicin to Quantify ChemoFilter Binding and Whole-Body Positron Emission Tomography/Magnetic Resonance for Drug Biodistribution

Parth Kumar, MD, **Colin Yee, BS**, **Joseph E. Blecha, MS**, **Thomas R. Hayes, PhD**, **Bridget F. Kilbride, BS**, **Carol Stillson, RVT**, **Aaron D. Losey, MD, MS**, **Eric Mastria, MD, PhD**, **Caroline D. Jordan, PhD, MS**, **Tony L. Huynh, BS**, **Terilyn Moore, BS, RT**, **Mark W. Wilson, MD**, **Henry F. VanBrocklin, PhD**, **Steven W. Hetts, MD**

Department of Radiology & Biomedical Imaging, University of California, San Francisco.

Abstract

Purpose: To evaluate radiolabeled doxorubicin (Dox) analogs as tracers of baseline Dox biodistribution in vivo during hepatic intra-arterial chemotherapy and to assess the efficacy of ChemoFilter devices to bind Dox in vitro.

Materials and Methods: In an in vitro static experiment, [fluorine-18]N-succinimidyl 4-fluorobenzoate ([^{18}F]SFB) and [fluorine-18]fluorobenzoyl-doxorubicin ([^{18}F]FB-Dox) were added to a beaker containing a filter material (Dowex resin, single-stranded DNA (ssDNA) resin, or sulfonated coated mesh). In an in vitro flow model, [^{18}F]FB-Dox was added into a Dox solution in phosphate-buffered saline, and the solution flowed via a syringe column containing the filter materials. In an in vitro flow experiment, using micro-positron emission tomography (PET), images were taken as [^{18}F]SFB and [^{18}F]FB-Dox moved through a phantom. For in vivo biodistribution testing, a catheter was placed into the common hepatic artery of a swine, and [^{18}F]FB-Dox was infused over 30 seconds. A 10-minute dynamic image and three 20-minute static images were acquired using 3T PET/MR imaging.

Results: In the in vitro static experiment, [^{18}F]FB-Dox demonstrated 76.7%, 88.0%, and 52.4% binding to the Dowex resin, ssDNA resin, and coated mesh, respectively. In the in vitro flow model, the first-pass binding of [^{18}F]FB-Dox to the Dowex resin, ssDNA resin, and coated mesh was 76.7%, 74.2%, and 76.2%, respectively, and the total bound fraction was 80.9%, 84.6%, and 79.9%, respectively. In the in vitro flow experiment using micro-PET, the phantom demonstrated a greater amount of [^{18}F]FB-Dox bound to both filter cartridges than of the control [^{18}F]SFB. In in vivo biodistribution testing, the first 10 minutes depicted [^{18}F]FB-Dox moving through the right upper quadrant of the abdomen. A region-of-interest analysis showed that the relative amount increased by 2.97 times in the gallbladder and 1.08 times in the kidney. The amount decreased by 0.74 times in the brain and 0.57 times in the heart.

Address correspondence to S.W.H., Department of Radiology and Biomedical Imaging, University of California, San Francisco, 185 Berry St., Suite 350, San Francisco, CA 94107; Steven.Hetts@ucsf.edu.

Conclusions: [^{18}F]FB-Dox can be used to assess Dox binding to ChemoFilters as well as in vivo biodistribution. This sets the stage for the evaluation of ChemoFilter efficacy in reducing toxicity due to intra-arterial chemotherapy.

Hepatocellular carcinoma (HCC) is the third-leading cause of cancer-related deaths worldwide. Transarterial chemo-embolization (TACE) is a standard of care for nonresectable HCC (1,2). Doxorubicin (Dox) is a chemotherapeutic agent frequently employed in TACE and has been shown to be highly effective against HCC, with a linear dose-response curve (3,4). However, Dox is session- and lifetime dose-limited because of its systemic toxicities, including cardiac failure (5).

ChemoFilter is a new intravascular device that uses specialized membranes or coatings to bind and remove a target drug from the circulation (6–9). ChemoFilters placed in the hepatic veins reduced the amount of Dox taken up by the heart and other organs outside the liver during TACE in a swine model (9). However, the reliable extraction of Dox from the ChemoFilter's binding surface is yet to be realized because of its high affinity for Dox, making the direct quantitation of Dox bound to the ChemoFilter device (and thus, removed from the body) challenging.

Prior literature has shown that there is a benefit of using ChemoFilter in vivo; it decreases the amount of Dox deposited in the heart, the site of dose-limiting toxicity (9). Although this result can be used to claim that ChemoFilter removes Dox, it is an indirect measurement of the filter's function. The most rigorous demonstration that Chemo-Filter binds to Dox in the hepatic veins during the intra-arterial infusion of Dox in the hepatic artery was performed to directly quantify the amount of Dox bound to the filter after the intra-arterial chemotherapy (IAC) procedure.

In this study, a radioactive Dox analog, [fluorine-18] fluorobenzoyl-doxorubicin ([^{18}F]FB-Dox) was used as a surrogate to assess the trapping properties of 2 ChemoFilter resin devices. Preliminary, in vivo positron emission tomography-magnetic resonance (PET/MR) imaging was performed to visualize and quantify the biodistribution of [^{18}F]FB-Dox in a swine model immediately after the intrahepatic artery injection of [^{18}F]FB-Dox.

MATERIALS AND METHODS

The filter materials tested were a porous, nylon-mesh cylinder (NITEX 03–250/50; Sefar AG, Heiden, Switzerland), with 250-μm pores to promote adequate diffusion, coated with a sulfonated polystyrene polymer; Dowex 50Wx2 50–100 Mesh (H) cation exchange resin (Dow Chemical Company, Midland, Michigan); and a customized single-stranded DNA (ssDNA) resin (Bioneer, Daejeon, South Korea) (10). The experiments were conducted in a radioactive safety hood. Phosphate-buffered saline (PBS; 1M), pH 7.4, was purchased from Life Technologies, Carlsbad, California.

Preparation of N-succinimidyl 4-[^{18}F] fluorobenzoate ([^{18}F]SFB) and [^{18}F]FB-Dox

The preparation of the prosthetic labeling groups [^{18}F]SFB and [^{18}F]FB-Dox was performed using modifications of previously reported procedures (11–14). All chemicals were

purchased from commercial sources and used without further purification. The ^{18}F ion, prepared on the University of California, San Francisco, PETtrace cyclotron (GE Healthcare, Chicago, Illinois) based on the ^{18}O(p,n)^{18}F reaction, was loaded onto the ELIXYS FLEX/CHEM automated production system (Sofie Biosciences, Dulles, Virginia) and trapped on a QMA cartridge (Waters, Milford, Massachusetts). The ^{18}F ion was eluted using Kryptofix [2.2.2] and potassium bicarbonate and azeotropically dried with acetonitrile. A solution of 4-(ethoxycarbonyl)-N, N, N-trimethylanilinium trifluoromethane-sulfonate salt in acetonitrile was reacted with the ^{18}F ion, and the resulting [^{18}F]fluorinated ethyl ester was saponified with tetrapropylammonium hydroxide. Further reaction occurred with tetramethyl-O-(N-succinimidyl) uronium tetrafluoroborate to produce [^{18}F]SFB, which was sequentially diluted with 0.1% acetic acid, trapped on an Oasis HLB cartridge, washed with 0.1% acetic acid, and eluted into a second ELIXYS reactor with acetonitrile.

[^{18}F]SFB was dried and reacted with Dox hydrochloric acid and trimethylamine in dimethylformamide at 30°C. [^{18}F]FB-Dox was purified using reverse-phase high-performance liquid chromatography. The purified tracer was then concentrated using a Sep-Pak C-18 Plus Light cartridge, eluted, and formulated in PBS or 5% ethanol. [^{18}F] FB-Dox was prepared with a decay-corrected yield of 12.7% ± 5.9 (n = 4, 0.6–1.6 GBq) in 129 minutes from the ^{18}F ion.

In Vitro Static Experiments

At time = 0, 3.145 MBq of [^{18}F]FB-Dox and 870 μCi of [^{18}F]SFB were added to a beaker containing 20 mL of PBS and a filter device (Dowex resin, ssDNA resin, sulfonated coating on mesh) to produce a total of 6 solutions. Each solution was equilibrated using a glass magnetic stirrer over a period of 30 minutes. One mL of each solution was sampled after 30 minutes to measure the amount of radioactivity remaining in the supernatant. The radioactivity was adjusted to account for decay, and the percentage bound to each resin was calculated based on the initial amount of radioactivity added.

In Vitro Flow Model

Single-pass flow experiments were conducted with both the radiotracers, [^{18}F]SFB and [^{18}F]FB-Dox. For the flow experiment, at time = 0, 100 μL of a compound was added to 3 mL of 0.05-M native Dox in PBS and flowed via a syringe column at a flow rate of 1 mL/min. The solution was passed through the filter 3 times, and the trapped amount was assessed after each successive pass through the filter device (Dowex, ssDNA resin, coating on polyethylene terephthalate mesh). After each pass, 100 μL was removed to quantify the remaining radioactivity. The experiment was conducted 3 times to account for variability. The radioactivity was adjusted to account for decay, and the percentage bound to each resin was calculated based on the initial amount of radioactivity added.

In Vitro Flow Experiment in Micro-PET

Additional Materials.—The additional materials were a standard 60-mL syringe infusion pump and the Inveon PET/computed tomography multimodality system (Siemens Healthineers, Knoxville, Tennessee) with a 1.6 × 1.6-mm detector pixel spacing, 1.4-mm spatial resolution, and 12.7-cm field of view.

Study Design.—A flow phantom was created using microtubing, 3 filter canisters, and two 60-mL syringes. Each phantom had 3 slots for each canister: 1 canister was a reservoir, and the other 2 canisters contained a filter device. One canister was used for a run with [^{18}F]SFB, the second was used for a run with [^{18}F]FB-Dox. The phantom was placed in a micro-PET scanner with tubing connecting the body to a syringe pump on either side. The circuit was primed with PBS. For [^{18}F]SFB and [^{18}F]FB-Dox, 10 μL at an initial rate of 1.3 MBqi/μL and 50 μL at an initial rate of 0.21 MBq/mL, respectively, was added to 50 mL of 0.05-M native Dox in PBS. The compound was then manually pushed through the syringe at a flow rate of 1 L/min.

The compound was passed though the phantom for 3 consecutive passes. Each pass was imaged using the Inveon micro-PET scanner (Siemens) to visualize the uptake of the radioactive compounds into the filter canisters. At the conclusion of the experiment, the amount of radioactivity in each filter canister, the reservoir, each syringe, and the liquid solution was quantified. The experiment was run once for each pair for a total of 4 times (Dowex + [^{18}F] SFB, Dowex + [^{18}F]FB-Dox, ssDNA resin + [^{18}F]SFB, ssDNA resin + [^{18}F]FB-Dox).

In Vivo Biodistribution Testing

A swine model with blood vessels and organs similar in size to those in adult humans was used to assess the baseline biodistribution of [^{18}F]FB-Dox in vivo, which acted as a control for when ChemoFilter is tested in the future. The study protocol was approved by the university's institutional animal care and use committee. Under general anesthesia, arterial access was obtained via a 6-F vascular sheath in the right common femoral artery. A 5-F Cobra catheter (Slip-Cath Beacon Tip; Cook, Bloomington, Indiana) was placed into the common hepatic artery of a single swine (37.0 kg, female) over a 0.035-inch guide wire using 30 × 30-cm^2, flat-panel, C-arm x-ray system guidance (Cios Alpha; Siemens Healthineers, Forchheim, Germany). An iodinated contrast agent was injected to view the gastroduodenal artery, which was then accessed using a 2.8-F Renegade Hi-Flo microcatheter (Boston Scientific, Marlborough, Massachusetts) and 0.014-inch Transend microwire (Stryker Neurovascular Division, Fremont, California). The contrast agent was injected to confirm placement. Three 3 × 20-mm Trufill coils (Cordis; Johnson, Miami, Florida) and four 10 × 100-mm Trufill coils (Johnson) were placed to occlude the gastroduodenal artery and, thus, prevent drug reflux. The microcatheter was removed, and the 5-F Cobra catheter was positioned in the common hepatic artery on a continuous heparinized salinedrip, distal to thehepaticartery bifurcation, as in a clinical IAC procedure. In parallel with the swine catheterization procedure, drug radiolabeling was performed in a radiation safety hood using 153 MBq of fluorobenzylamide Dox (half-life, 109 minutes) in 10 mL of 2-mg/mL Dox.

The swine was transported under general anesthesia from the C-arm room to the PET/MR room. A 3.0T PET/MR system (SIGNA; GE Healthcare, Waukesha, Wisconsin), with 16-channel upper and lower anterior array coils and a 14-channel posterior array coil, was used for the simultaneous acquisition of PET and MR imaging data. [^{18}F]FB-Dox was infused over a 30-second period, and then, simultaneous, 10-minute, time-of-flight (TOF) dynamic

PET and MR image data were acquired over the liver. The MR imaging sequences included a 3-dimensional, breath-held, fast spoiled gradient echo sequence (LAVA Flex) with an axial scan plane; a single-shot, fast spin-echo sequence with an axial scan plane; and a coronal single-shot, fast spin-echo sequence with fat saturation. Next, a 20-minute static TOF PET/MR image was acquired over the whole body using 5 beds that were 4 minutes each (total, 20 minutes per task) to encompass the entire pig. The beds were positioned to encompass the head, upper chest, lower chest, upper abdomen, lower abdomen/legs. The whole-body PET task was repeated 3 times to evaluate the distribution up to 90 minutes after infusion. The dynamic time points were selected because they were the earliest achievable scan times. Later time points were spaced at approximately 30, 60, and 90 minutes because these were time points used during prior research (9).

Data Analysis

A statistical analysis was conducted using Microsoft Excel (Microsoft Corporation, Redmond, Washington). The standard error was calculated and plotted. The 1-tailed t-test was conducted using Excel to determine the statistical significance in the quantitative flow experiment. For in vivo testing, the attenuated corrected images were converted to standardized uptake values. A region-of interest was manually drawn on a single 2-dimensional image (slice thickness, 898.40–976.55 μm), copied over to each corresponding time point to maintain a constant area, and the sum of the standardized uptake values was measured using Horos.

RESULTS

Preparation of [^{18}F]SFB and [^{18}F]FB-Dox

The radioactive tracers were prepared in the radiochemistry laboratory of the University of California, San Francisco. [^{18}F]SFB was prepared from ethyl 4-N,N,N-trimethy-lammonium benzoate salt on the ELIYXS automated synthesis system using previously described methods as shown in Figure 1 (11–13). [^{18}F]SFB is a pendant prosthetic group that has been used to radiolabel compounds with free amine groups. In this study, [^{18}F]SFB was applied as a nonbinding control compound. As also shown in Figure 1, [^{18}F]SFB was reacted with Dox to prepare [^{18}F]FB-Dox, a radiolabeled surrogate of Dox, to demonstrate trapping on the ChemoFilter resins.

In Vitro Static and Flow Experiments

The static experiment was conducted to ensure that a radioactive analog of Dox binds to ChemoFilter similar to native Dox. The radioactive analog and the radioactive prosthetic used to prepare the Dox radioactive tracer were exposed to the 3 filter materials (Dowex resin, ssDNA resin, and sulfonated coating) to assess binding. An in vitro flow experiment was conducted to introduce fluid dynamics after the compounds were shown to be able to bind to the filter devices in the static experiment. Single-pass flow experiments were conducted to allow each compound mixture to flow through each filter device once.

For the in vitro static experiment, the [^{18}F]SFB control had 0% ± 2 binding on all 3 filter devices. [^{18}F]FB-Dox demonstrated 76.7%, 88.0%, and 52.4% binding on the Dowex resin, ssDNA resin, and sulfonated coated mesh, respectively.

For the in vitro, single-pass flow experiment, the amount trapped by each filter device during the first pass and the total amount trapped after 3 passes were analyzed. The average first-pass binding value of [^{18}F]FB-Dox to the Dowex resin, ssDNA resin, and sulfonated coated mesh was 76.7% ± 2.9, 74.2% ± 4.2, and 76.2% ± 0.62, respectively. The average total binding value after 3 passes was 80.9% ± 1.5, 84.6% ± 4.8, and 79.9% ± 1.1, respectively. The binding value for each filter material was statistically significant between their respective first- and third-pass measurements (*P* values, .003, .030, and .034, respectively).

In Vitro Flow Experiments Using Micro-PET

An experiment was conducted to confirm whether the radioactive analogs of Dox can be visualized using PET imaging in a flow circuit. For this experiment, the goal was to determine whether the radioactive analog was visualized using the PET scanner and whether there was a difference in the amount of bound [^{18}F]SFB (control) and [^{18}F]FB-Dox. There was a greater amount of [^{18}F]FB-Dox bound to both the filter cartridges than that of [^{18}F]SFB during all 3 passes.

In Vivo Biodistribution Testing

For the in vivo experiment, the animal was given a hepatic artery infusion of [^{18}F]FB-Dox and monitored for 90 minutes. For the first 10 minutes, a dynamic TOF scan was performed. The radioactive compound was seen moving through the catheter, into the liver, and eventually into the gallbladder (seen at the bottom left of the 10th image in Fig 2). The overlay of the image is shown in coronal images in Figure 2. The region-of interest analysis conducted on Figure 2 is shown in the Table. The relative amount of radioactive compound increased by 2.97 times in the gallbladder, 1.42 times in bladder, and 1.08 times in the kidney. The amount decreased by 0.74 times in the brain, 0.57 times in the heart, and 0.42 times in the liver (Fig 3).

DISCUSSION

Prior studies have noted a benefit of introducing Chemo-Filters to the hepatic veins and vena cava during preclinical, in vivo, hepatic IAC trials, with a significant decrease in the amount of Dox deposited in the liver, heart, and kidney (6–9). Although these studies were able to show the benefit of ChemoFilter via blood sampling, they were unable to quantify the amount of Dox bound to ChemoFilter itself: the filter's high drug binding affinity prevented the re-elution of Dox for quantification.

The purpose of this study was to show that the radioactive analogs of Dox can be used as a surrogate to detect the amount of Dox bound to ChemoFilter and detect its overall biodistribution using PET/MR imaging. The first experiment of this study demonstrated that [^{18}F]FB-Dox bound to the Dowex and ssDNA resins and was trapped by the filter device to a similar degree as native Dox. There is 1 amine group on native Dox; this amine was

used for the synthesis of [^{18}F]FB-Dox. It is possible that the positive charge was diffuse over the conjugated structure and that [^{18}F]FB-Dox adhered to the Dowex resin via ionic interactions: the negatively charged Dowex resin presumably interacted with the positive charge. In contrast, the ssDNA resin likely bound to [^{18}F]FB-Dox via **π-π** bonding via the compound's benzene rings. [^{18}F]SFB does not have a conjugated benzene structure similar to Dox and served as a nontrapping control.

During the in vitro flow experiment, the ability of the filter system to adsorb the radioactive analog of Dox showed that the filter device does not need to be in static equilibrium for the radioactive analogs of Dox to bind to the filter. The flow experiment demonstrated that the majority of binding happens in the first pass through the filter: greater than 74% of the binding of [^{18}F]FB-Dox to all 3 filter devices occurred, with minimal increment in subsequent passes. This is true for both the ssDNA and Dowex filter devices. This is important for translation to clinical practice. Dox concentration will be highest in the blood in the hepatic veins and inferior vena cava (IVC) during the first pass of Dox through these veins during and immediately after Dox infusion in the hepatic artery. Similarly, Dox concentration exposed to the reactive surfaces of Chemo-Filters deployed in the hepatic veins and IVC will be highest during the first pass, before Dox has had an opportunity to be pumped through the heart and to organs throughout the body.

The flow experiment was scaled to account for the rate at which blood flows into the IVC. Although it may not scale appropriately, it establishes a benchmark for assessing various filter devices. It is interesting to note that the sul-fonated coated PET mesh filter device had a greater increase in binding during pass 2 compared with either of the other filter devices (Fig 4). This result could be due to the increased surface area that is seen, given that fluid can flow through the mesh but flows faster through the column because of increased porosity. Fluid flowing through the resin may move more slowly, given its decreased porosity, and will allow for more binding time. Compared with the static experiment, the PET mesh bound more [^{18}F]FB-Dox. Micro-PET confirmed the prior results and confirmed that [^{18}F]FB-Dox can be visualized using a micro-PET scanner (Fig 5). Both the filter devices tested showed increased uptake when [^{18}F]FB-Dox was pushed through the phantom compared with the control [^{18}F]SFB was used. As seen during the static experiment, the ssDNA filter device bound more [^{18}F]FB-Dox compared with the Dowex filter device. Although this experiment was not quantitative, one can visually detect the qualitative increase in the amount of compound bound to the filter cartridges.

In the in vivo experiment, PET/MR image acquisition demonstrated the biodistribution of [^{18}F]FB-Dox over time during a simulated IAC procedure, as a proxy for native Dox. As shown in Figure 2, there was an increase in the signal in the right hepatic lobe during the first 2 minutes, likely due to the injection catheter being angled toward the right hepatic artery. However, near the end of the 10 minutes, in the last 3 dynamic PET images, there was an increase in the signal in the gallbladder. In addition, the static PET/MR sequences showed the amount of [^{18}F]FB-Dox increasing primarily in the gallbladder because it is filtered through the liver as well as in the bladder because it is filtered from the bloodstream (Fig 3). The negative trend in the heart is most likely due to the body's own blood filtration systems. However, in comparison with the brain, there was an increased amount of Dox deposited

in the heart (Fig 6), thus underscoring the potential utility of ChemoFilter in preventing cardiac deposition. It is also notable that the majority of radioactivity measured was near the infusion site in the liver (and the gallbladder) and not in remote organs such as the heart (Table).

There are several limitations to this study. A significant limitation of this study is the small number of repetitions in the swine model. Because of coronavirus disease 2019 restrictions at the institution, additional large-animal imaging experiments could not be conducted. However, a breadth of preliminary PET/MR imaging data was obtained from the first swine model. In addition, this study did not assess the in vitro testing of the specific version of the ChemoFilter device used in the previous study (9). This was also limited by the closure of the research laboratory during the coronavirus disease 2019 pandemic. ChemoFilter may be a promising method for removing Dox from the systemic circulation to reduce toxicity due to TACE procedures. However, quantifying its efficacy has been challenging, particularly because young swines do not experience the same cardiac toxicities as adult humans with cancer.

A radioactive analog of Dox was studied and found to be capable of binding to several known Dox-specific filter types. [^{18}F]FB-DOX was also shown to be visualized using a PET/MR scanner and can be used to assess the bio-distribution of native Dox. This will allow the assessment of relative changes throughout the body with the addition of endovascular filtration devices. Thus, [^{18}F]FB-Dox presents a new method for the quantification of the systemic distribution of Dox in vivo via PET imaging, with or without the use of ChemoFilter.

Acknowledgments

C.Y. and H.F.V. were supported by a grant from the National Institutes of Health (R01 CA194533). S.W.H. received grant support for the study from the National Institutes of Health (R01 CA194533), Siemens, and Stryker; receives consulting fees from Imperative, Route 92, Cerenovus, and Kaneka; serves on an advisory board of Cerenovus; holds 2 patents and 1 pending patent related to ChemoFilter technology; holds a potential equity position in Filtro Inc, a startup that will commercialize ChemoFilter; and has received payments for expert testimonies. None of the other authors have identified a conflict of interest.

ABBREVIATIONS

Dox	doxorubicin
[^{18}F]FB-Dox	[fluorine-18]fluorobenzoyl-doxorubicin
[^{18}F]SFB	[fluorine-18]N-succinimidyl 4-fluorobenzoate
HCC	hepatocellular carcinoma
IAC	intra-arterial chemotherapy
IVC	inferior vena cava
MR	magnetic resonance
PBS	phosphate-buffered saline

PET	positron emission tomography
ssDNA	single-stranded DNA
TACE	transarterial chemo-embolization
TOF	time-of-flight

REFERENCES

1. Budny A, Kozłowski P, Kamińska M, et al. Epidemiology and risk factors of hepatocellular carcinoma. Pol Merkur Lekarski 2017; 43:133–139. [PubMed: 28987047]
2. Pinheiro PS, Callahan KE, Jones PD, et al. Liver cancer: a leading cause of cancer death in the United States and the role of the 1945–1965 birth cohort by ethnicity. JHEP Reports 2019; 1:162–169. [PubMed: 32039366]
3. El-Kareh AW, Secomb TW. Two-mechanism peak concentration model for cellular pharmacodynamics of doxorubicin. Neoplasia 2005; 7: 705–713. [PubMed: 16026650]
4. Lencioni R, Petruzzi P, Crocetti L. Chemoembolization of hepatocellular carcinoma. Semin Intervent Radiol 2013; 30:3–11. [PubMed: 24436512]
5. Shi Y, Moon M, Dawood S, McManus B, Liu PP. Mechanisms and management of doxorubicin cardiotoxicity. Herz 2011; 36:296–305. [PubMed: 21656050]
6. Aboian MS, Yu JF, Gautam A, et al. In vitro clearance of doxorubicin with a DNA-based filtration device designed for intravascular use with intra-arterial chemotherapy. Biomed Microdevices 2016; 18:1–9. [PubMed: 26660457]
7. Patel AS, Saeed M, Yee EJ, et al. Development and validation of endovascular chemotherapy filter device for removing high-dose doxorubicin: preclinical study. J Med Device 2014; 8:041008.
8. Oh HJ, Aboian MS, Yi MY, et al. 3D printed absorber for capturing chemotherapy drugs before they spread through the body. ACS Cent Sci 2019; 5:419–427. [PubMed: 30937369]
9. Yee C, McCoy D, Yu J, et al. Endovascular ion exchange chemofiltration device reduces off-target doxorubicin exposure in a hepatic intra-arterial chemotherapy model. Radiol Imaging Cancer 2019; 1:e190009. [PubMed: 32300759]
10. Jawad B, Poudel L, Podgornik R, Steinmetz NF, Ching WY. Molecular mechanism and binding free energy of doxorubicin intercalation in DNA. Phys Chem Chem Phys 2019; 21:3877–3893. [PubMed: 30702122]
11. Lazari M, Collins J, Shen B, et al. Fully automated production of diverse 18F-labeled PET tracers on the ELIXYS multireactor radiosynthesizer without hardware modification. J Nucl Med Technol 2014; 42:203–210. [PubMed: 25033883]
12. Wüst F, Hultsch C, Bergmann R, Johannsen B, Henle T. Radiolabelling of isopeptide Nε-(γ-glutamyl)-L-lysine by conjugation with N-succinimidyl-4-[18F]fluorobenzoate. Appl Radiat Isot 2003; 59:43–48. [PubMed: 12878121]
13. Mäding P, Füchtner F, Wüst F. Module-assisted synthesis of the bifunctional labelling agent N-succinimidyl 4-[18F]fluorobenzoate ([18F] SFB). Appl Radiat Isot 2005; 63:329–332. [PubMed: 15949940]
14. Kumar P, Watts A, Acharya P, et al. Radiosynthesis of [18F]-fluorobenzoate-doxorubicin using acylation approach. Curr Radiopharm 2016; 9:215–221. [PubMed: 27237136]

RESEARCH HIGHLIGHTS

- The ChemoFilter device has been developed to absorb excess doxorubicin in the hepatic veins during hepatic intra-arterial chemotherapy before the drug can distribute throughout the body and cause off-target side effects.
- In vitro, the ChemoFilter device bound to the radioactive analogs of doxorubicin at a similar level as that bound to nonradioactive doxorubicin.
- In vivo, the baseline distribution of radioactive doxorubicin analogs in a swine model was measured using positron emission tomography/magnetic resonance imaging during and after hepatic artery infusion.

STUDY DETAILS

Study type: Laboratory study/Animal study

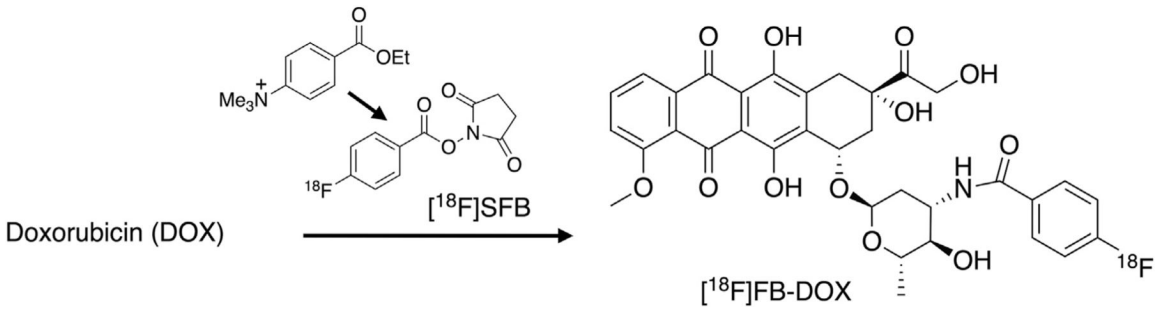

Figure 1.

Preparation of succinimidyl [Fluorine-18]fluorobenzoate and [Fluorine-18]fluorobenzoyl-doxorubicin. [^{18}F]FB-Dox = [Fluorine-18]fluorobenzoyl-doxorubicin; [^{18}F]SFB = [Fluorine-18]fluorobenzoate.

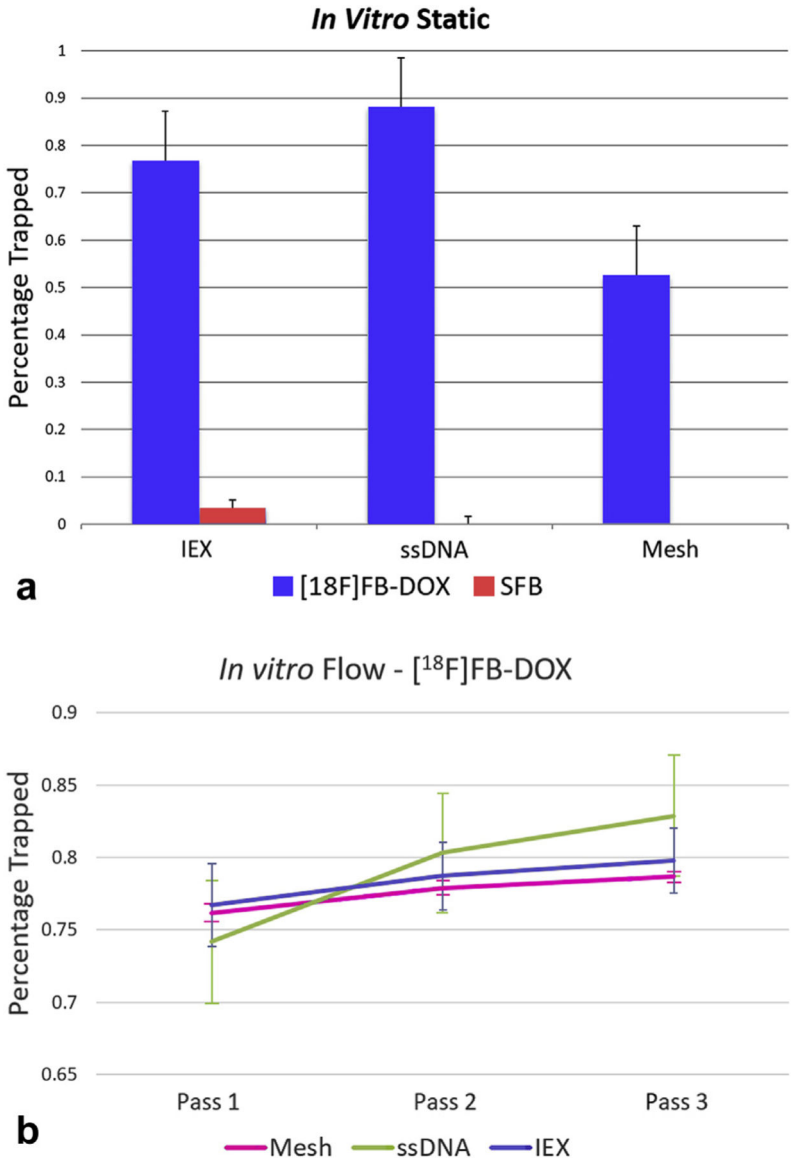

Figure 2.

Dynamic time-of-flight positron emission tomography and simultaneous magnetic resonance imaging over 10 minutes (with 1 frame per minute), from top left to bottom right.

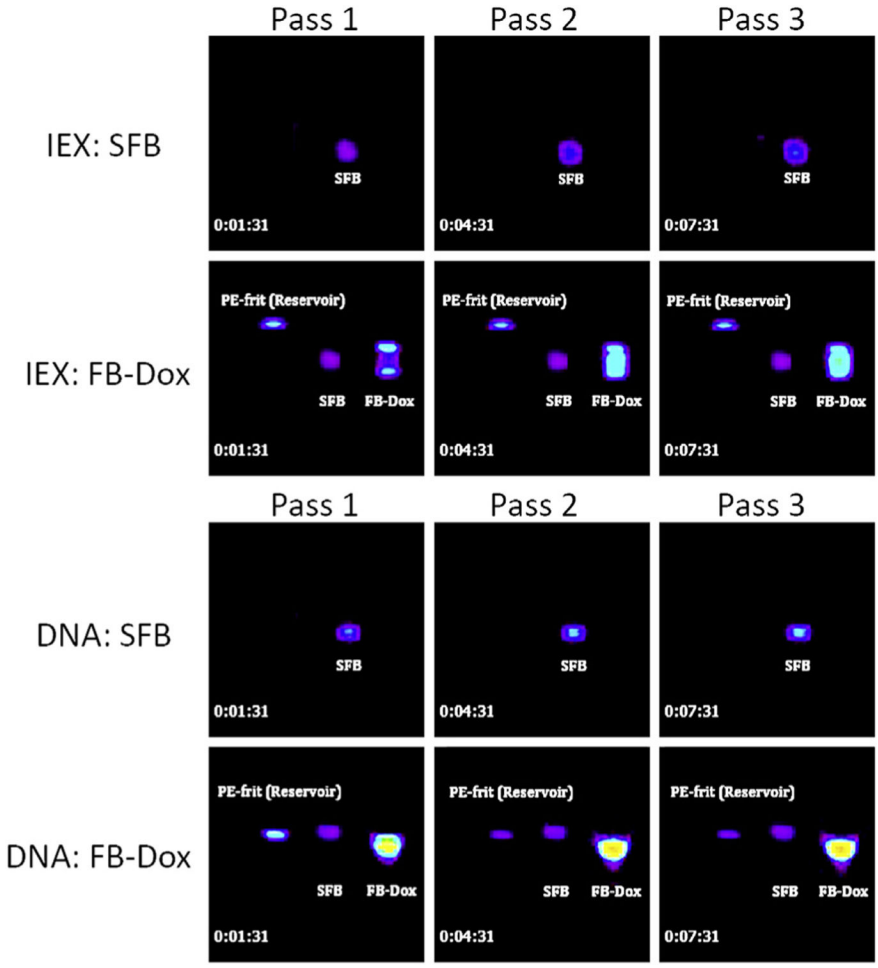

Figure 3.

Static time-of-flight positron emission tomography and simultaneous magnetic resonance imaging was acquired at 10, 36, 62, and 88 minutes (left to right). Shown are positron emission tomography standardized uptake value images, with 30 maximum-intensity projection images overlaid on the LAVA Flex magnetic resonance imaging sequence.

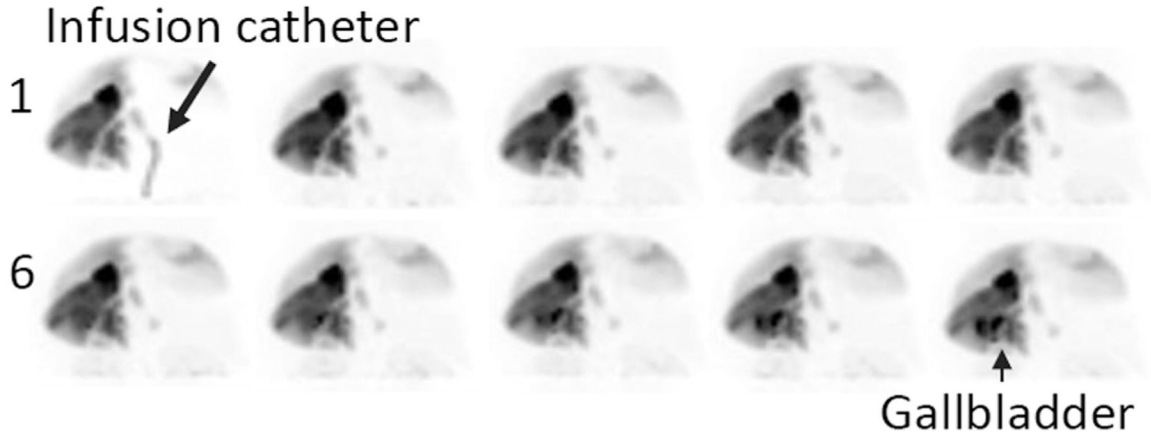

Figure 4.

(a) Comparison of the relative trapping of each radioactive compound to each filter device within a static environment. **(b)** Comparison of the relative trapping of 3 filter devices with [Fluorine-18]fluorobenzoyl-doxorubicin through 3 consecutive passes. [^{18}F]FB-Dox = [Fluorine-18]fluorobenzoyl-doxorubicin; [^{18}F]SFB = [Fluorine-18]succinimidyl fluorobenzoate; IEX =; ssDNA = single-stranded deoxyribonucleic acid

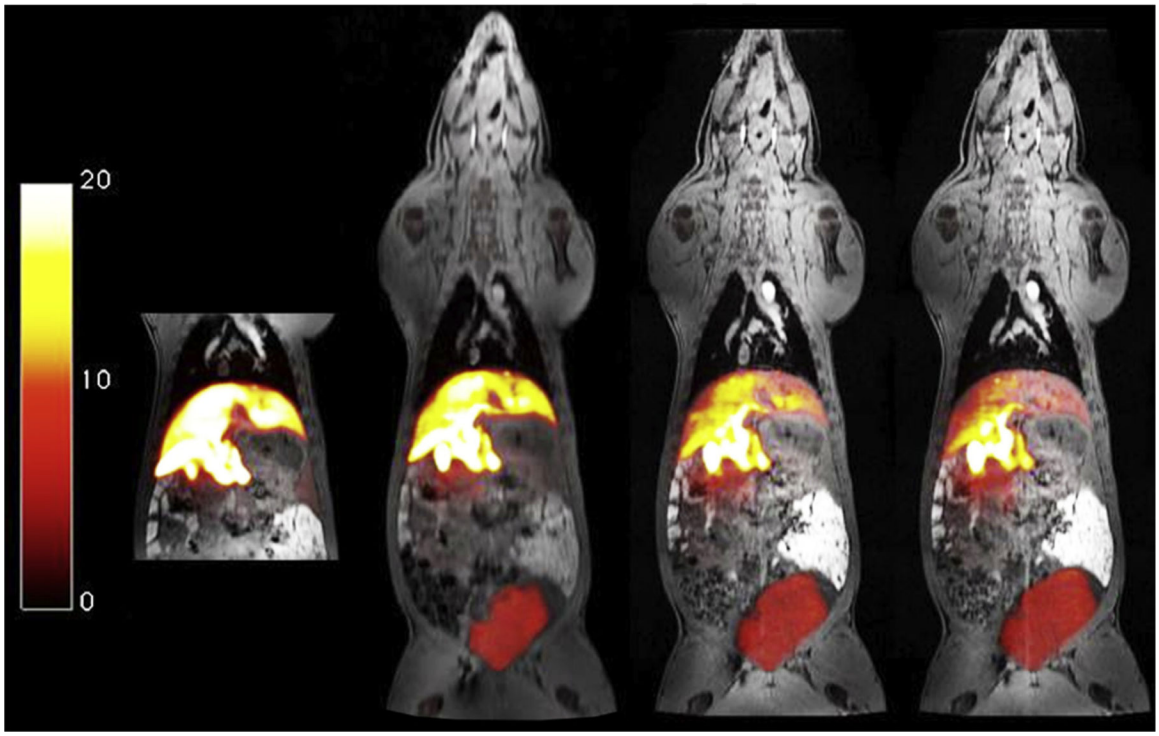

Figure 5.

Using a micro-positron emission tomography scanner, a phantom with 4 different pairs of radioactive analogs and filter devices was imaged. Each pair was imaged over 3 passes. [^{18}F]FB-Dox = [Fluorine-18]fluorobenzoyl-doxorubicin; IEX =; [^{18}F]SFB = [Fluorine-18]succinimidyl fluorobenzoate.

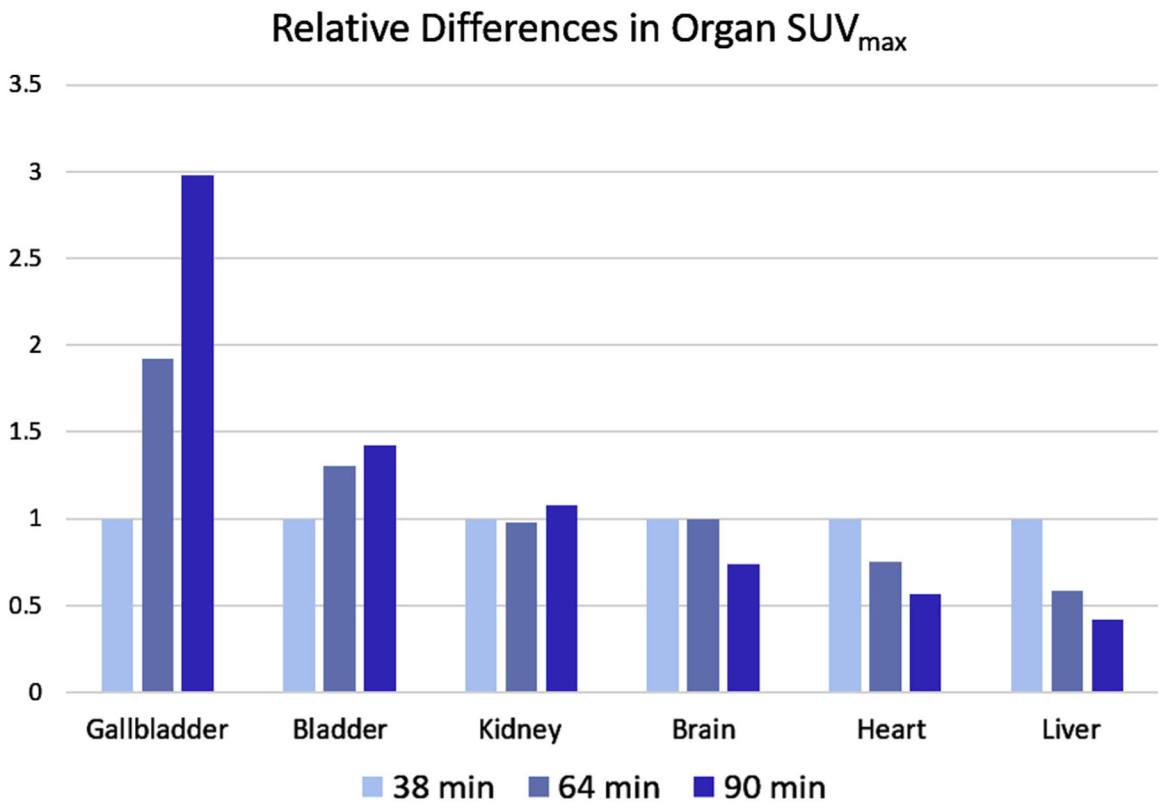

Figure 6.

Standardized uptake value $(SUV)_{sum}$ single-slice region-of-interest analysis performed on positron emission tomography SUV images shown in Figure 4, normalized to their respective 36-minute SUV value. SUV = standardized uptake value.

Table.

Absolute Standardized Uptake Value of Each Organ at the Specified Time point Used for Figure 5.

Organ	36 min.	62 min.	88 min.
Gall bladder	17,999	34,593	53,567
Bladder	3,853	5,020	5,477
Kidney	1,489	1,456	1,608
Brain	27	27	20
Liver	15,545	9,141	6,531
Heart	432	325	245